Morphology, Thermal Property, and Mechanical Property of Core–Shell Latex Polymers. I. Effect of Heating and Pressuring on PBA/PS Linear Composite Polymer

CHIA-FEN LEE, YU-HSIA CHEN, WEN-YEN CHIU

Department of Chemical Engineering, National Taiwan University, Taipei, Taiwan, Republic of China

Received 29 March 1996; accepted 30 October 1997

ABSTRACT: In this work, butyl acrylate and styrene were used as monomers in the first stage and second stage of polymerization, respectively, and potassium persulfate ($K_2S_2O_8$) was used as the initiator to synthesize the poly(butyl acrylate)–polystyrene (PBA/PS) composite latex by the method of two-stage soapless emulsion polymerization. The morphology of the latex particles was observed by transmission electron microscopy (TEM), which showed that the composite latex particles had a core–shell structure. The particle-size distribution of the composite latex was very uniform. A thin layer of a PBA-*graft*-PS copolymer was formed in between the core (PBA) and shell (PS) regions, which thus increased the compatibility between the PBA and PS phases. The process of heating and pressuring influenced the morphology, mechanical properties, and thermal properties of the PBA/PS composite polymer. © 1998 John Wiley & Sons, Inc. J Appl Polym Sci 69: 13–23, 1998

Key words: core–shell; morphology; thermal property; mechanical property; composite polymer

INTRODUCTION

To extend the applicability of polymers, blending is one of the efficient ways to achieve this aim. But the degree of mixing or compatibility between two polymers varies very much with the blending process, which influences the final properties of the polymer blends. In recent years, many articles[1–6] studied the synthesis of composite latex or latex IPN to improve the degree of compatibility between the two polymer phases.

By the method of seeded emulsion polymerization, a core–shell polymer/polymer composite latex was synthesized.[7–9] The core–shell structure improved the interfacial adhesion and enhanced the compatibility between the two polymer phases of the composite in comparison with the conventional polymer blends.

There were many factors to control the kinetics and morphology of polymer particles during emulsion polymerization, such as the method of monomer fed into the system,[10,11] the sequence of monomers fed into the system, the monomer ratio in the two stages, the hydrophilicity of the monomers, the surface tension, the molecular weight of the polymers,[11–13] the compatibility of the polymers,[14] and the properties of the initiators.[15]

The effects of heating on the thermal and mechanical properties of a PBA/PS composite latex were studied by Chen et al.[16,17] They pointed out that the PS continuous phase would dissolve in the PBA phase with increasing annealing temperature. Besides, they found that the effects of heating on the morphology showed that one partial PS phase dissolved in the PBA phase and the other partial PS continuous phase coagulated and

Correspondence to: W.-Y. Chiu.

Journal of Applied Polymer Science, Vol. 69, 13–23 (1998)
 CCC 0021-8995/98/010013-11

formed the larger size dispersed in the PBA phase. The effect of heating on the mechanical property showed that the tensile strength and modulus decreased and the breaking elongation increased with increasing annealing temperature.

The advantages of soapless emulsion polymerization are its potential to form uniform latex particles and the avoidance of pollution from the emulsifiers. But the latex can become unstable in the condition of high solid content without the protection of an emulsifier on the latex particles. Therefore, the solid content of the soapless emulsion system was usually low in order to keep the emulsion stable throughout the reaction.

In this work, styrene was the polymerized, which formed the PBA/PS core–shell composite latex. The purpose of this work was to investigate the extent of grafting between PBA and PS. Then, the variations of the morphology, thermal property, and mechanical property of the polymer obtained from the composite latex upon heating and pressuring were examined and discussed. All of them could be correlated quite well.

EXPERIMENTAL

Materials

Butyl acrylate and styrene were distilled under a nitrogen atmosphere and reduced pressure prior to polymerization. Water was redistilled and deionized. Other chemicals were of analytical grade and used without further purification.

Ingredients and Conditions for Polymerization

In the first stage, PBA seed latex was synthesized via soapless emulsion polymerization. The ingredients and conditions for the synthesis of the seed latex are given below:

Butyl acrylate (g)	130
Initiator ($K_2S_2O_8$) (g)	0.866
Deionized water (g)	1300
Temperature (°C)	70
Stirring rate (rpm)	300
Reaction method	Batch
Solid content (g/L H_2O)	100

In the second stage, styrene was polymerized in the presence of the PBA seed latex. The ingredients and conditions for the synthesis of the PBA/PS composite latex are given below:

Seed latex (g)	500
Styrene (g)	90.91
Initiator ($K_2S_2O_8$) (g)	0.5, 1
Temperature (°C)	70, 80
Stirring rate (rpm)	300, 500
Reaction method	Batch
Solid content (g/L H_2O)	300

Polymerization

As mentioned above, in the first stage of the reaction, the synthesis of the PBA seed latex was carried out at 70°C. The stirring rate was controlled at 300 rpm. The reaction went on for 1 h and the polymerization reaction of the first stage was complete; then, the seed latex was quenched to room temperature. In the second stage of the reaction, the latex seeds were first swollen with quantitative styrene for 24 h at room temperature. Then, the reaction system was heated to the reaction temperature; with the addition of $K_2S_2O_8$, the second stage of the reaction started.

Conversion

At a certain time interval during the second stage of polymerization, a sample of the emulsion latex was taken out of the reactor and poured into methanol with hydroquinone to stop the reaction. The precipitated polymers were washed with methanol and water several times and then dried in a vacuum oven.

The conversion in the second stage of the reaction was calculated as follows:

$$\text{Conversion } (x) = \frac{W_2 - W_1 \times B\ \%}{W_1 \times M_0\ (\text{ST})\ \%}$$

where W_1 is the weight of sample taken from the vessel; W_2, the weight of dry polymers obtained from the taken sample; M_0 (ST) %, the initial weight percentage of the styrene monomer in the reaction mixture; and B %, the weight percentage of PBA in the reaction mixture.

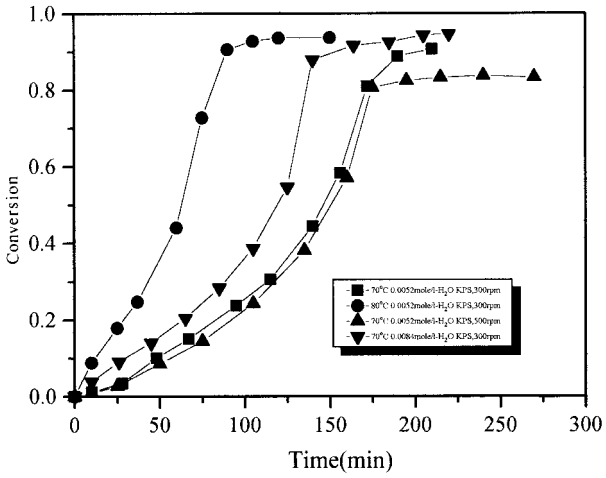

Figure 1 Conversion versus reaction time at different reaction temperatures, initiator concentrations, and agitation speeds.

Thin-layer Chromatographic (TLC) Analysis[18]

Qualitative Analysis

The polymers obtained from the PBA/PS composite latex, PBA latex, and PS latex were each dissolved in tetrahydrofuran (THF) to prepare the polymer solutions with a concentration of 0.005 g/mL. One microliter of each polymer solution was taken out and dripped onto the TLC plates. After effluxion with the appropriate solvent, CCl_4/$CH_3COOC_2H_5$, in a weight ratio of 85/15, the TLC plates were sprayed with a solution of Thymol Blue in a water–ethyl alcohol mixture. Then, the H_2SO_4 at a concentration of 10*N* was sprayed onto the TLC plates. Finally, the TLC plates with the polymers were dried in the oven.

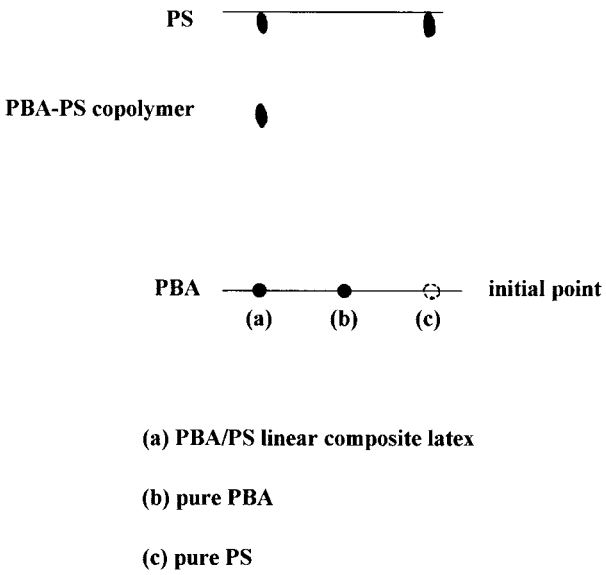

Figure 2 TLC figures of PBA, PS, and PBA/PS composite polymers.

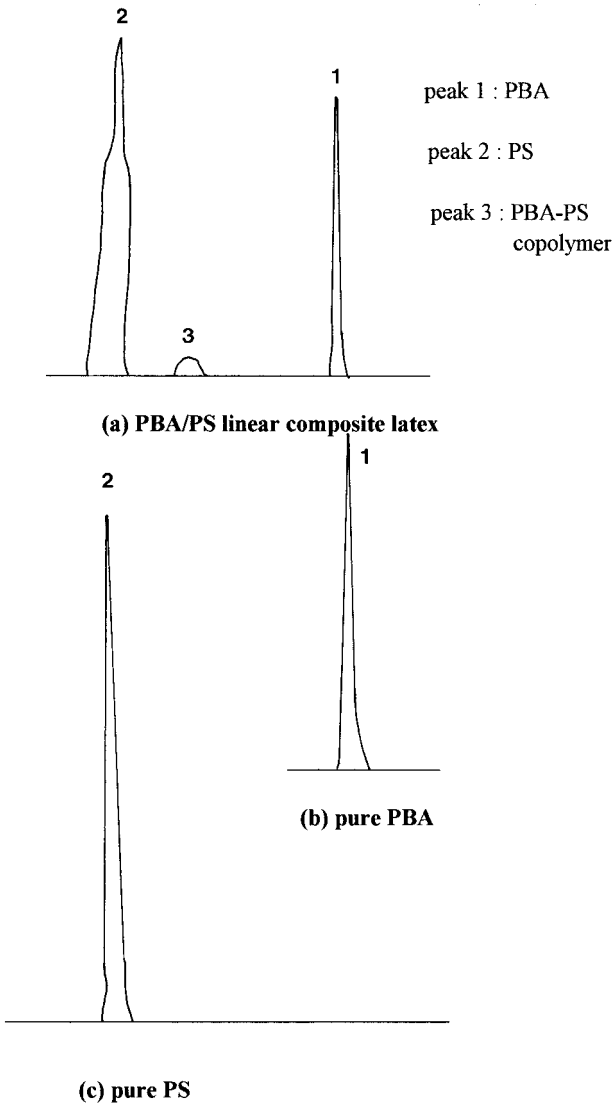

Figure 3 TLC–FID figures of PBA, PS, and PBA/PS composite polymers.

Quantitative Analysis

The samples were quantitatively analyzed by the TLC/flame ionization detector (FID) method. One microliter of the polymer solution of the sample in THF was dripped onto a thin quartz rod coated with a silica gel 75 μm thick. The polymer components in the sample were separated with appro-

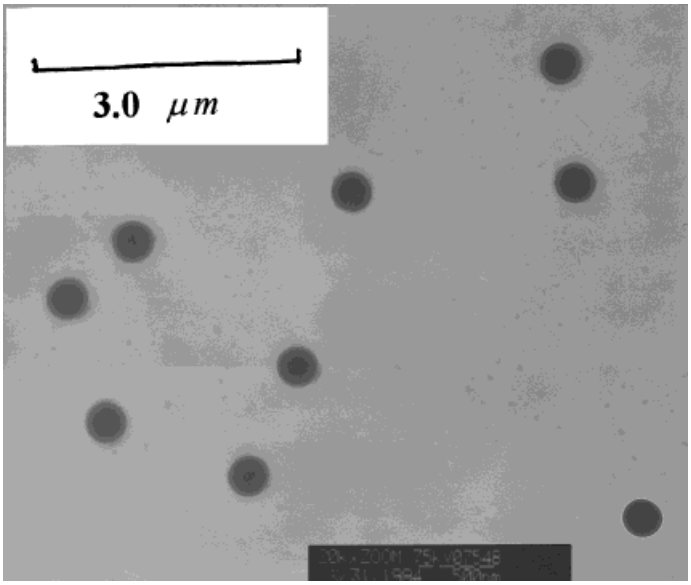

Figure 4 TEM photograph of PBA/PS composite latex (magnification = ×10 K).

priate solvents as mentioned in the prior subsection. At the end, the composition of the samples on the rods was measured by the FID.

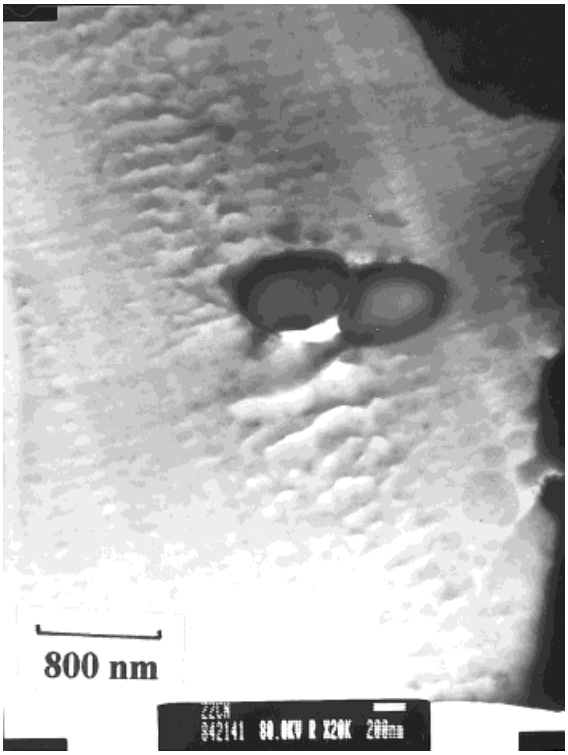

Figure 5 TEM photograph of the stained cross sections of PBA/PS composite latex particles (magnification = ×20 K).

Observation of Particle Morphology[8,9]

Apparent Morphology of Latex Particles Observed Under the TEM

The latex particles from the seeded polymerization were taken out from the reactor and the apparent morphology of the latex particle was examined under the TEM.

Inner Morphology of Latex Particles Observed Under the TEM

The latex particles from the seeded polymerization were ultramicrotomed and stained with RuO_4. The stained sections of the latex particles were observed under the TEM.

Morphology of Latex Polymer After Processing Observed Under the TEM

The latex particles were washed with methanol and water several times and dried, then processed to form a block of sample. The sample was ultramicrotomed and stained with RuO_4. The stained sections of the sample were observed under the TEM.

Dynamic Mechanical Analysis (DMA)

The polymers obtained from the composite latex were hot-pressed to prepare the DMA testing samples. The DMA measurements were run un-

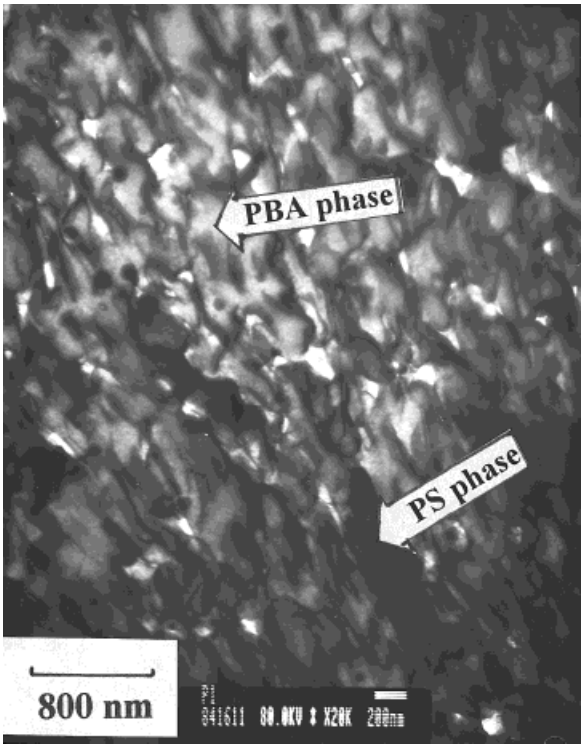

Figure 6 TEM photograph of the stained cross section of the PBA/PS composite polymer which was hot-pressed under 140°C and 140 psi for 10 min (magnification = ×20 K).

der the heating rate of 5°C/min, frequency of 1 Hz, and amplitude of 0.2 mm. The results of the DMA measurement showed the values of log E', log E'', and tan δ; the peak temperature of log E'' was taken as the glass transition temperature (T_g) of the sample.

Mechanical Property

The polymers obtained from the composite latex were hot-pressed to prepare the tensile-testing samples. The tensile strength of the samples was measured by a Universal testing instrument under the tensile rate of 10 mm/min at room temperature.

RESULTS AND DISCUSSION

Conversion

This study was to investigate the effects of the reaction temperature, agitation speed, and initiator concentration on the reaction rate, but the BA/ST monomer ratios remained constant. Figure 1 shows the effects of the reaction temperature, initiator concentration, and agitation speed on the conversion during the course of the reaction. It appeared that the conversion was higher under the conditions of higher temperature, higher initiator concentration, or lower agitation speed over the entire course of the polymerization. The reduction of conversion under a higher agitation speed was because the monomer droplets were broken into smaller sizes, created more surface areas, and increased the probability of capturing radicals from the aqueous phase. On the contrary, the concentration of radicals captured by the polymer particles decreased. Because the reaction site of the polymerization was in the polymer particles, the decrease of the radical concentration would, thus, slow down the reaction rate in the polymer particles. The reason for the final conversion of less than 100% was due to the glassy effect. When the glass transition temperature of the polymer particles was higher than the reaction

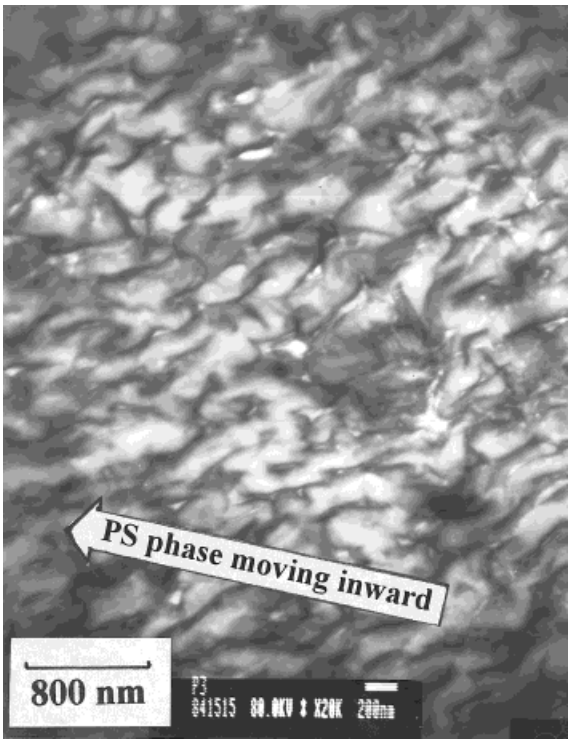

Figure 7 TEM photograph of the stained cross section of the PBA/PS composite polymer which was hot-pressed under 140°C and 140 psi for 30 min (magnification = ×20 K).

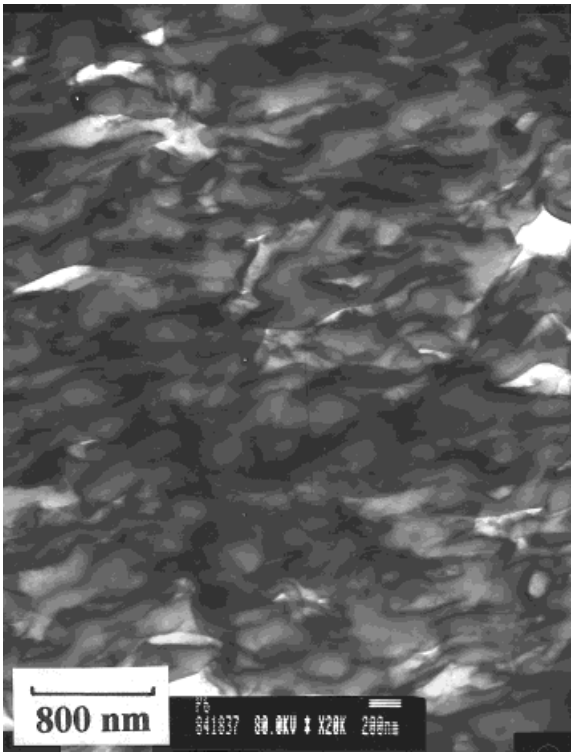

Figure 8 TEM photograph of the stained cross section of the PBA/PS composite polymer which was hot-pressed under 140°C and 140 psi for 1 h (magnification = ×20 K).

temperature (70°C), the monomer propagation was difficult to continue in the polymer particles; thus, the final conversion could not reach 100%.

TLC Analysis

Qualitative Analysis

Figure 2 shows the results of the TLC analysis for PBA, PS, and the PBA/PS polymer obtained from its respective emulsion latex. Pure PBA stayed at the original point, and pure PS traveled over 8 cm from the original place. Also, the PBA/PS composite polymer decomposed into three components, at the original place, 5 cm from the original place, and 8 cm from the original place respectively. This finding indicated that a thin layer of the PBA-*graft*-PS copolymer formed in between the core (PBA) and shell (PS) regions for the PBA/PS latex particles.

Quantitative Analysis

Figure 3 shows the results of the TLC–FID analysis for the PBA/PS composite polymer obtained from its emulsion latex. Three peaks appeared, corresponding to the PBA, PBA-*graft*-PS, and PS components. The area of each peak was proportional to the weight content of each component. So, from the area calculation of the three peaks for PS, PBA, and PBA-*graft*-PS, the weight percentage of PBA-*graft*-PS was estimated to be 4.6% for the PBA/PS composite polymer. The grafting layer between the core and shell regions was very thin.

Morphology

Morphology of PBA/PS Composite Latex

Figure 4 is a TEM photograph of the PBA/PS composite latex particles. The diameter of the composite latex particles was very uniform, around 446.7 nm, which implied that no new particles were formed during the second-stage reaction. In the second-stage reaction, the number of the seed latex particles was 5.7×10^{15} L/L H_2O, and the average diameter of the seed latex particles was 305 nm. If the average size of the secondary nucleation did not occur through the second stage of the reaction, the final composite particles were estimated to be 452 nm, which was very close to the value measured from the TEM. Therefore, it was certain that the secondary nucleation was negligible throughout the second stage of the reaction. Figure 5 is a TEM photograph of the stained cross section of the PBA/PS composite latex particles, which showed the core–shell structure; the lighter region is PBA and the darker region is the PS shell.

Effect of the Pressure on the Morphology of PBA/PS Composite Polymer

Figures 6–8 are TEM photographs which show the effects of heat and pressure on the morphology of the PBA/PS composite polymer. In this experiment, the temperature and pressure were fixed at

Table I Surface Tension of PS and PBA[19]

	Surface Tension (dyne/cm)		
	20°C	140°C	180°C
PS	40.7	32.1	29.2
PBA	33.7	25.3	22.5

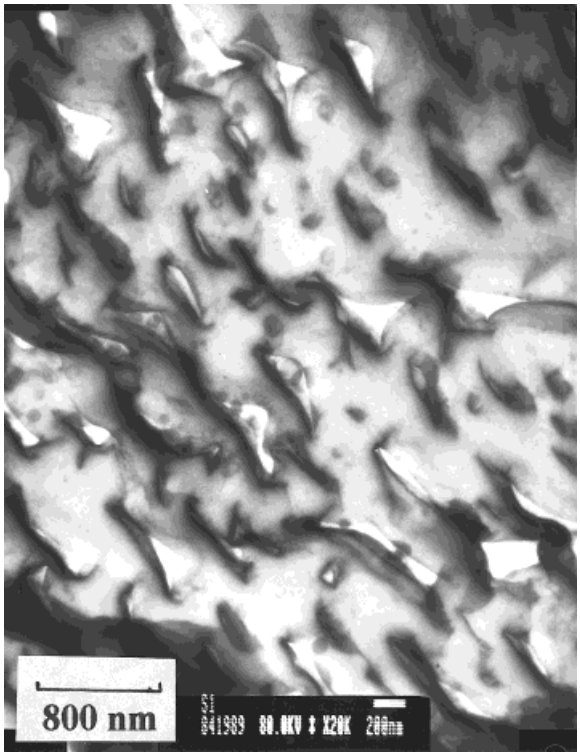

Figure 9 TEM photograph of the stained cross section of the PBA/PS composite polymer which was extruded from the capillary rheometer under a shear rate of 5.74 L/s and 200°C (magnification = ×20 K).

140°C and 140 psi, respectively. Figure 6 shows the morphology of the PBA/PS composite polymer after heating and pressuring for 10 min. The dispersed phase (bright zone) is PBA and the continuous phase (dark zone) is PS. The boundary between the PBA and PS phases is irregular, indicating that a low interfacial tension exists in between and that the grafting layer plays a key role in it. Figure 7 shows the morphology of the PBA/PS composite polymer after heating and pressuring for 30 min. It appeared that the PBA phase and the PS phase were gradually mixed with each other. The PBA phase in the core region was dispersing, and the PS phase in the shell region was moving inward gradually (the arrow in Fig. 7 shows the PS phase moving inward). Both PBA and PS form a transient and interpenetration state. After heating and pressuring for 1 h, as shown in Figure 8, the PS phase was concentrated together significantly, and a phase inversion in some regions of the composite is shown. Because the heat and pressure further lowered the interfacial tension, the PBA phase and the PS surface could easily interpenetrate each other. The PS phase with a higher surface tension than that of the PBA phase then was gradually centered together and pushed PBA outward. Therefore, the phase inversion was observable somewhere in this sample. Table I shows the surface tension of PS and PBA, respectively, at different temperatures.[19] The surface tension of PBA and PS both decreased with increasing temperature, and PS had a larger surface tension. All the data gave support to our above explanation.

Figures 9 and 10 shows TEM photographs of the morphology of the PBA/PS composite polymers under the effects of shear and high temperature. The composite polymer showed a phase-inversion morphology, in which the PS coagulated to form the dispersed phase, and the PBA was spread over to form the continuous phase. The phase inversion was more profound under a higher shear rate as seen in Figure 10. Because the high temperature lowered the interfacial ten-

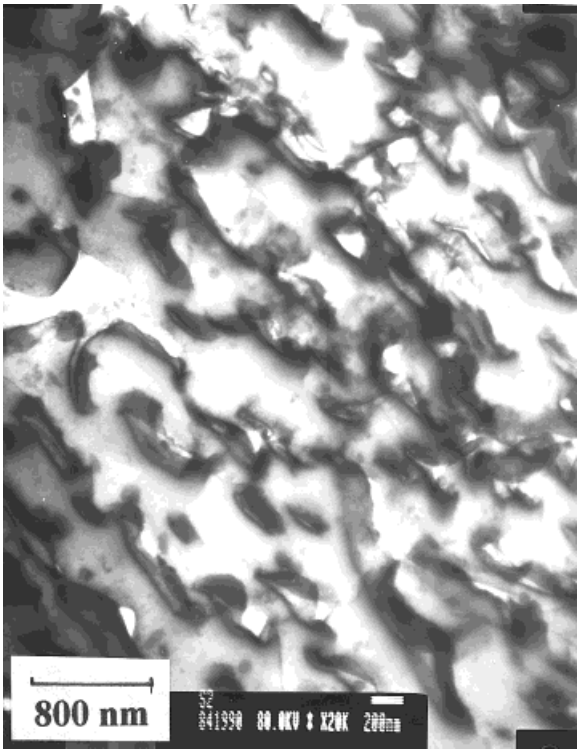

Figure 10 TEM photograph of the stained cross section of the PBA/PS composite polymer which was extruded from the capillary rheometer under a shear rate of 1185 L/s and 200°C (magnification = ×20 K).

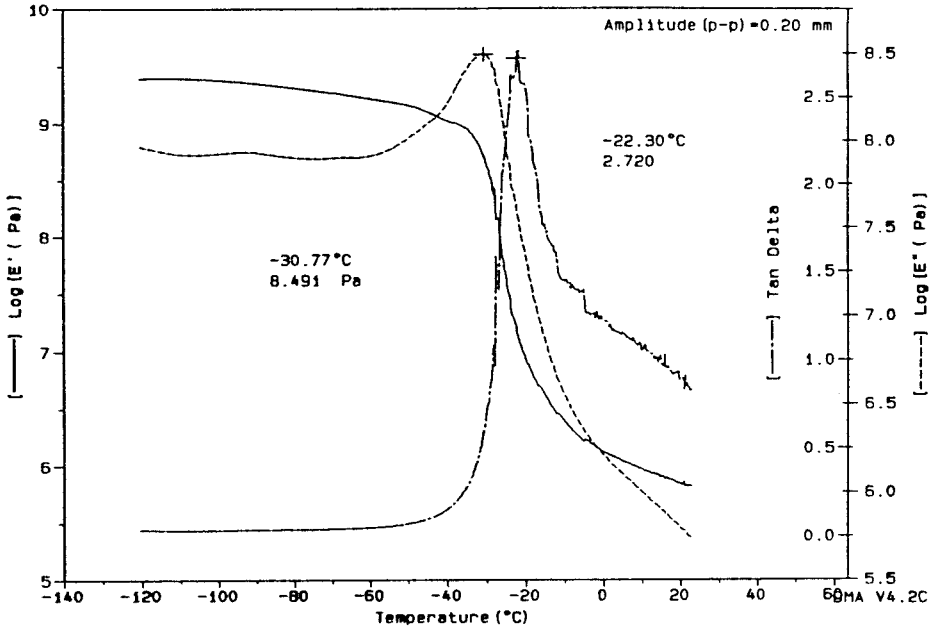

Figure 11 DMA curve of PBA seed latex polymer.

sion between PBA and PS, and the high shear further accelerated the phase interpenetration, finally resulting in a phase inversion by the fact that PS has a higher cohesive energy than that of PBA.

Thermal Property of PBA/PS Composite Polymer Under Heat and Pressure

Figure 11 shows the DMA curve of the PBA seed latex polymer, and Figures 12–14 shows the DMA

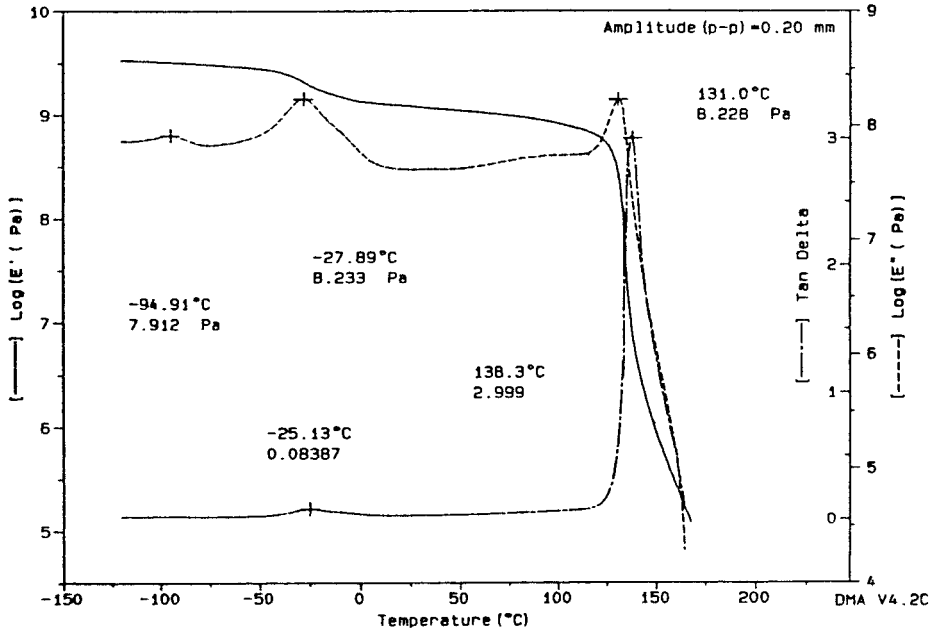

Figure 12 DMA curve of PBA/PS composite polymer which was hot-pressed at 140°C and 140 psi for 10 min.

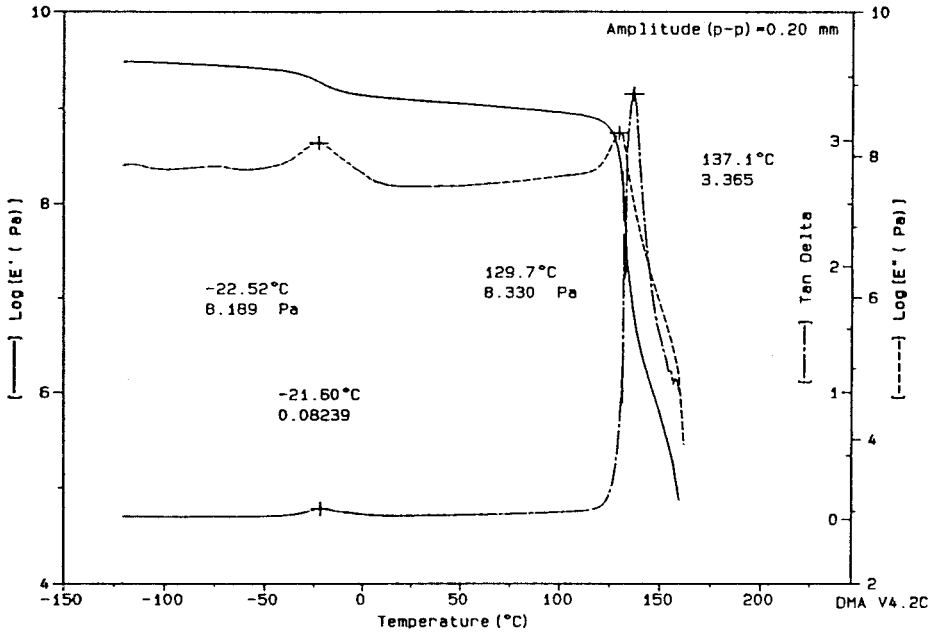

Figure 13 DMA curve of the PBA/PS composite polymer which was hot-pressed at 140°C and 140 psi for 30 min.

curves of the PBA/PS composite polymer after the process of heating and pressuring. The composite polymer was hot-pressed at 140°C and 140 psi for 10 min, 30 min, and 1 h, respectively, before the DMA test. The T_g's shown on the DMA curves are summarized in Table II. It shows that the T_g of pure PBA obtained from the seed latex in the first stage of the reaction was −30.77°C. After hot-pressing for 10 min, the T_g of the PBA phase in the PBA/PS composite polymer shifted to −27.89°C; the degree

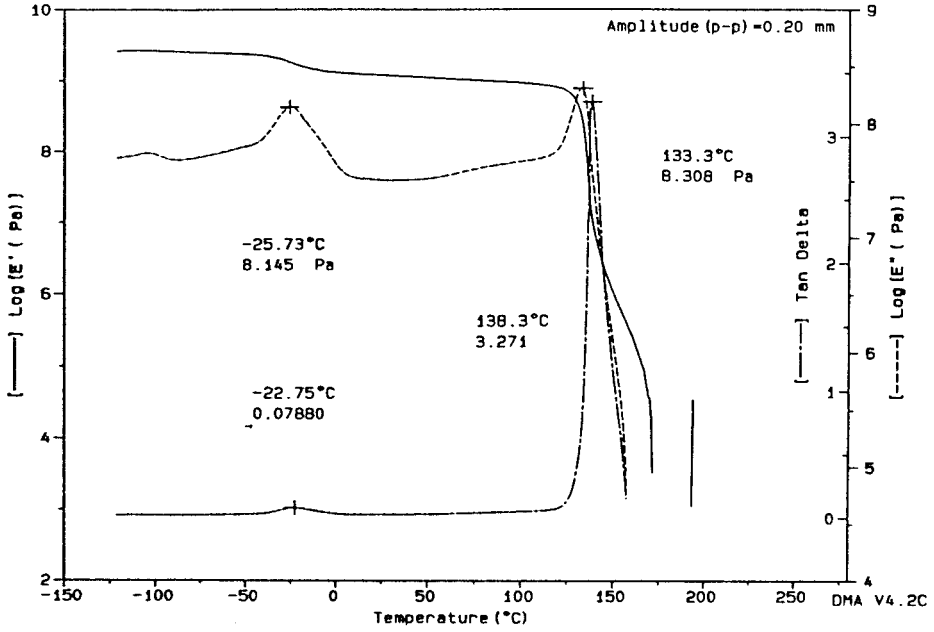

Figure 14 DMA curve of PBA/PS composite polymer which was hot-pressed at 140°C and 140 psi for 1 h.

Table II Effect of Hot-pressing on the T_g of the PBA/PS Composite Polymer

Time for Hot-pressing	T_g's of PBA/PS: BA Phase T_g (°C)	T_g's of PBA/PS: PS Phase T_g (°C)	T_g of PBA Seed	Degree of Shift of T_g for PBA Phase
10 min	−27.89	131	−30.77	2.88
30 min	−22.52	129.7	−30.77	8.25
1 h	−25.73	133.3	−30.77	5.04

of the shift was 2.88°C. As mentioned above, the thin layer of the PBA-*graft*-PS copolymer in the boundary of the core and shell regions increased the degree of compatibility between the PBA and PS phases, so that the T_g of the PBA phase shifted toward a higher temperature. With increasing the time of hot-pressing, the degree of shift would be more significant. As seen in Table II, the T_g of the PBA phase shifted to −22.52°C after 30 min of hot-pressing in which the PBA chains and PS chains gained enough energy to disturb and interpenetrate each other, so the degree of the shift was larger. However, after 1 h of hot-pressing, the T_g of the PBA phase shifted back to −25.73°C; the degree of the shift was smaller than that processed for 30 min. It was due to the phase inversion that we discussed in the section titled Morphology, and the phase separation gradually became more apparent again.

Mechanical Properties of PBA/PS Composite Polymer Under Heat and Pressure

Table III shows the tensile strength, elongation, and Young's modulus of the PBA/PS composite polymer under the influence of heating and pressure. The composite polymer was hot-pressed at 140°C and 140 psi. After processing for 30 min, the tensile strength, elongation, and Young's modulus of the composite polymer were higher than those processed for 10 min, due to that the degree of interpenetration among PBA and PS chains increased to some extent under the hot press for 30 min, which was also reflected in the degree of the shift of the T_g. But when the composite polymer was processed for 1 h or longer, phase inversion gradually occurred, the PS phase was concentrated together, and the phase separation became more obvious. So, the tensile strength, elongation, and Young's modulus of the composite polymer decreased, indicating that the mechanical behavior of the composite polymer under heat and pressure could be well elucidated from the change of its morphology.

Table III Effect of Hot-pressing on the Mechanical Properties of the PBA/PS Composite Polymer

Time for Hot-pressing (min)	Tensile Strength (N/mm^2)	Young's Modulus (N/mm^2)	Elongation (%)
10	10.46	300.5	3.46
30	12.72	355.13	3.46
60	10.48	316.34	3.31

CONCLUSIONS

In this work, PBA/PS composite latex was synthesized by the method of a two-stage soapless emulsion polymerization. The first stage was to synthesize the PBA seed latex and the second stage was to synthesize the PS in the presence of PBA seeds. In the second stage of polymerization, an increase of the reaction temperature or initiator concentration or a reduction of the agitation speed would increase the reaction rate. The core–shell morphology of the PBA/PS composite latex particles was observed by TEM with the PBA phase as the core and the PS phase as the shell. A thin layer of the PBA-*graft*-PS copolymer was formed in the boundary of the core region and the shell region, which increased the degree of compatibility of the PBA phase and the PS phase. The morphology, thermal properties, and mechanical properties of the PBA/PS composite polymer under the process of heating and pressuring were investigated. The T_g's and mechanical properties were related to the morphology of the composite polymer, that is, the degree of interpenetration between the PBA and

PS phases, which increased first and then decreased with increasing processing time.

REFERENCES

1. K. Shibayama and Y. Suzuki, *Rubb. Chem. Tech.,* **40,** 476 (1967).
2. D. Klempner, *Angew. Chem.,* **90,** 104 (1978).
3. H. A. J. Battaerd, *J. Polym. Sci.,* **49c,** 149 (1975).
4. D. S. Kaplan, *J. Appl. Polym. Sci.,* **20,** 2615 (1976).
5. R. E. Touhsaent, D. A. Thomas, and L. H. Sperling, *J. Polym. Sci.,* **46,** 175 (1974).
6. L. H. Sperling, *Polym. Eng. Sci.,* **16,** 87 (1976).
7. C. F. Lee, K. R. Lin, and W. Y. Chiu, *J. Appl. Polym. Sci.,* **51,** 1621 (1994).
8. C. F. Lee and W. Y. Chiu, *J. Appl. Polym. Sci.,* **56,** 1263 (1995).
9. C. F. Lee and W. Y. Chiu, *J. Appl. Polym. Sci.,* **57,** 591 (1995).
10. J. L. Jonsson, H. Hassande, L. H. Jonsson, and B. Tornell, *Macromolecules,* **24,** 126 (1991).
11. T. I. Min, A. Klein, M. S. El-Aasser, and J. W. Vanderhoff, *J. Polym. Sci. Polym. Chem. Ed.,* **21,** 2845 (1983).
12. D. I. Lee and T. Ishikawa, *J. Polym. Sci. Polym. Chem. Ed.,* **21,** 147 (1983).
13. R. A. Dickie, M. F. Cheung, and S. Newman, *J. Appl. Polym. Sci.,* **17,** 65 (1973).
14. D. J. Hourston, R. Satgurunthan, and C. H. Varma, *J. Appl. Polym. Sci.,* **31,** 1955 (1986).
15. I. Cho and K. W. Lee, *J. Appl. Polym. Sci.,* **30,** 1903 (1985).
16. D. Chen, Q. Wang, G. Huang, and J. Zhang, *Polym. Mater. Sci. Eng.,* **Jan.**(1), 58 (1993).
17. D. Chen, Q. Wang, and G. Huang, *Polym. Mater. Sci. Eng.,* **Mar.**(2), 51 (1993).
18. T. I. Min, A. Klein, M. S. El-Aasser, and J. W. Vanderhoff, *J. Polym. Sci.,* **21,** 2845 (1983).
19. S. Wu, *Polymer Interface and Adhesion,* New York and Basel, 1982.